

## INTRASEASONAL OSCILLATIONS AND THE SOUTH CHINA SEA SUMMER MONSOON ONSET

WEN ZHOU<sup>†</sup> and JOHNNY C. L. CHAN\*

*Laboratory for Atmospheric Research Department of Physics and Materials Science City University of Hong Kong, Hong Kong, China*

*Received 25 July 2004*

*Revised 20 April 2005*

*Accepted 20 April 2005*

### ABSTRACT

This paper investigates the role of intraseasonal oscillations (ISOs) in the onset of the South China Sea summer monsoon (SCSSM). Two major components of ISO (10–20-day and 30–60-day modes) are identified. The coupling of these two intraseasonal modes during the pre-monsoon period of the SCSSM are investigated by examining the filtered outgoing longwave radiation (OLR), low-level circulation, apparent heat source and apparent moisture sink from October of a previous calendar year to September of a calendar year.

The zonal and meridional propagations of the 10–20-day and 30–60-day modes are found to be different, which reflects their different roles in the establishment and development of the SCSSM. The northwestward propagation of the 10–20-day mode is associated with the weakening of the subtropical high over the western Pacific, while the northeastward propagation of the 30–60-day mode originates from convection over the equatorial Indian Ocean. A hypothesis is then proposed to explain the observed variabilities in the SCSSM onset. When the equatorial Indian Ocean exhibits a 30–60-day mode oscillation, an initially weak convection develops into a large convection band (or monsoon trough). Meanwhile, a convective disturbance of the 10–20-day mode is induced when this monsoon trough extends to the western Pacific. These two processes then collaborate to cause a weakening of the subtropical anticyclone over the South China Sea. Because the monsoon trough associated with the 30–60-day mode subsequently propagates northward into the Bay of Bengal (BOB), the induced vortex together with the 10–20-day westward-migrating convection from the equatorial western Pacific will substantially increase the effect of horizontal advection of moisture and heat, thus destabilizing the atmosphere and weakening the subtropical ridge there. Westerlies can then penetrate and prevail over the SCS region, and the SCSSM onset occurs. Copyright © 2005 Royal Meteorological Society.

KEY WORDS: intraseasonal oscillations; South China Sea summer monsoon; monsoon onset

### 1. INTRODUCTION

A general conclusion on the South China Sea summer monsoon (SCSSM) onset is that it is associated with a switch of the zonal winds over the South China Sea (SCS) from easterly to westerly, and accompanied by an increase in convective activity (e.g. Wu *et al.* 1999a; Xu and Chan, 2001). Previous studies have shown that the intraseasonal oscillations (ISOs) can substantially affect the monsoon system Chen *et al.*, 2000. Madden and Julian (1971) first observed a 40–50-day oscillation (the Madden–Julian Oscillation, or MJO) by analyzing zonal wind anomalies in the tropical Pacific. Murakami *et al.* (1986) suggested that the ISO might be responsible for the monsoon onset. Lau and Chan (1986) discussed the 30–60-day mode in association with the monsoon trough/ridge. Chen and Chen (1995) demonstrated a kind of 30–60-day mode in the summer monsoon circulation of the SCS–western tropical Pacific region during 1979. Sometimes the term ‘MJO’ is used interchangeably with the tropical ‘ISO’. However, the ISO consists of more than the

\* Correspondence to: Johnny C. L. Chan, Department of Physics and Materials Science, City University of Hong Kong, Tat Chee Ave., Kowloon, Hong Kong, China; e-mail: Johnny.Chan@cityu.edu.hk

<sup>†</sup> Current Address: Institute of Atmospheric Physics, Chinese Academy of Sciences, Beijing, China

MJO. It has been shown to have another popular timescale (10–20-day mode (some authors refer to it as the biweekly mode, or even a broadband 10–30-day mode)) besides the 30–60-day (some authors refer to it as the 40–50-day, or even a broadband 20–72-day) mode (Krishnamurti and Bhalme, 1976; Yasunari, 1979; Wang and Rui, 1990; Chen and Chen, 1993; Chan *et al.*, 2002). The 10–20-day mode has been suggested to contribute to the Indian summer monsoon (Krishnamurti and Ardanuy, 1980) and the SCSSM (Chen and Chen, 1993, 1995; Chan *et al.*, 2002; Mao and Chan, 2005), and exhibits a double-cell structure along the Indian monsoon trough and along the equator (Chen and Chen, 1993, 1995). The northward-propagating 30–60-day mode is also found to be present in the monsoon trough/ridge (Lau and Chan, 1986; Lau and Yang, 1997).

Furthermore, a SCSSM break apparently occurs simultaneously with a phase lock between the 30–60-day and the 10–20-day modes over the northern SCS (Chen and Chen, 1995). On the basis of the data from the South China Sea Monsoon Experiment (SCSMEX) in 1998, Chan *et al.* (2002) observed that the maintenance and break of the 1998 SCSSM were controlled by the 30–60-day oscillation and further modified by the 10–20-day mode. Recently, Mao and Chan (2005) extended their study and proposed that the 30–60-day and 10–20-day mode oscillations control the behavior of the SCSSM activities for most years. The 30–60-day oscillation of the SCSSM exhibits a trough–ridge seesaw over the SCS, with anomalous cyclones (anticyclones) along with enhanced (suppressed) convection migrating northward. On the other hand, the 10–20-day oscillation manifests as an anticyclone/cyclone system over the western tropical Pacific with a largely zonal orientation propagating westward into the SCS.

Most of the previous works on the ISO associated with the SCSSM focused on the development and maintenance of the SCSSM. The present study attempts to investigate the role of the ISO (10–20-day and 30–60-day modes) in the pre-monsoon period of the SCSSM, and the following questions are addressed: (i) is the ISO also significant during the pre-monsoon period as in the monsoon period? (ii) are these two oscillations the dominant modes leading to the SCSSM onset? (iii) what are the possible mechanisms responsible for these two oscillations contributing to the SCSSM onset? (iv) is the ISO a potential predictable factor for the onset/end cycle and active/break cycle of the SCSSM?

Data and methodology are first introduced in Section 2. Features associated with the 10–20-day and 30–60-day modes are then presented in Section 3. The role of the ISO activities in the onset and the evolution of SCSSM are examined in Section 4. The relationship between the ISO and the El Niño/Southern Oscillation (ENSO) is then discussed in Section 5. Concluding remarks are given in Section 6.

## 2. DATA AND METHODOLOGY

### 2.1. Data

The data used in this study are mainly from the National Centers for Environmental Prediction (NCEP) reanalysis II. These include the daily mean values of geopotential height, wind speed, air temperature, and specific humidity from 1979 to 2001. Daily outgoing longwave radiation (OLR) data from the National Oceanic and Atmospheric Administration for 25 years from 1979 to 2001 are also used. The horizontal resolution of these data is 2.5° latitude/longitude square.

### 2.2. Methodology

Distributions of  $Q_1$  (apparent heat source) and  $Q_2$  (apparent moisture sink) are used as basic variables to examine the seasonal variability of land–sea thermal contrast, the definitions of which are:

$$Q_1 = C_p \left[ \frac{\partial T}{\partial t} + \vec{V} \cdot \nabla T + \left( \frac{p}{p_0} \right)^{\frac{R}{C_p}} \cdot \omega \cdot \frac{\partial \theta}{\partial p} \right] \quad (1)$$

$$Q_2 = -L \left[ \frac{\partial q}{\partial t} + \vec{V} \cdot \nabla q + \omega \cdot \frac{\partial q}{\partial p} \right] \quad (2)$$

where  $T$  is the air temperature,  $\theta$  the potential temperature,  $R$  and  $C_p$  the gas constant and the specific heat at constant pressure of dry air respectively,  $\vec{V}$  the vector wind,  $\omega$  vertical  $p$ -velocity,  $q$  specific humidity,  $L$  the latent heat of condensation,  $p$  the pressure, and  $p_0$  the surface pressure.

The lagged regression analysis is very useful in examining the evolution of ISO in the tropical atmosphere if a nearly linear relationship between convection and circulation exists (e.g. Matthews and Kiladis, 1999). On the basis of such an assumption, the tropical heating is linearly correlated with OLR and the response to this heating can be illustrated by linear dynamics (e.g. Matthews and Kiladis, 1999). Although nonlinear processes such as conditional instability of the second kind are also important in the tropics (e.g. Chang and Lim, 1988), many researchers have found some evidence to demonstrate that realistic flow perturbations in the tropics can be obtained by forcing linear barotropic models with steady, divergent sources (Webster, 1972; Simmons, 1982; Simmons *et al.*, 1983; Mureau *et al.*, 1987; Chelliah *et al.*, 1988).

Given a reference time series  $x_t$ , the  $lag(\Delta t)$  is regressed by the linear, least-square fitting when the dependent variable  $y_t$  leads  $x_t$  by  $\Delta t$  day (s)

$$y_{t+\Delta t} = \hat{y}_{t+\Delta t} + \ell_{t+\Delta t} = ax_t + b + \ell_{t+\Delta t} \quad (3)$$

where  $a$  is the coefficient of slope,  $b$  the intercept, and  $\ell_{t+\Delta t}$  the residual. Thus, the  $lag(\Delta t)$  regression map against convection on the onset day describes the atmospheric condition  $\Delta t$  day(s) before or after deep convection occurs in the SCS domain.

In order to investigate the relationship between ISO and SCSSM, a 'reference' time series {in this study, the 10–20-day or 30–60-day filtered  $OLR_{i,j}$  [ $1 \leq i \leq 181$  (90 days before and after the onset date),  $1 \leq j \leq 22$  (year 1980–2001)] averaged over the SCS domain} is chosen as the independent variable. Then the dependent variables (the total number  $N = i \times j = 3982$ ), such as filtered wind,  $Q_1$ , and  $Q_2$ , are regressed against the 'reference' timeseries. Finally, a  $t$ -test with  $N - 2$  degrees of freedom is used to determine whether the correlations between the two variables are significant:

$$t = \frac{r/\sqrt{N-2}}{\sqrt{1-r^2}} \quad (4)$$

where,  $r$  is the correlation coefficient, and  $N$  the total number ( $N = i \times j = 3982$ ).

### 3. CHARACTERISTICS OF THE ISO

#### 3.1. Wavelet analysis of OLR anomalies over the SCS

In this study, 181 days [90 days before and after the onset date, see Table I – the onset pentad defined as the first pentad after mid-April when the 5-day mean value of the 850-hPa zonal winds is westerly over the central and southern part of the SCS (110–120°E, 5–15°N) and lasts for more than two pentads] of OLR anomalies averaged over the SCS are chosen each year. Writing  $OLR_{i,j}$  as the OLR on the  $i$ -th day of the  $j$ -th year [ $1 \leq i \leq 181$  (90 days before and after the onset date),  $1 \leq j \leq 22$  (year 1980–2001)], the composite mean OLR can be defined as

$$O\hat{L}R_i = \frac{1}{22} \sum_{j=1}^{22} OLR_{ij} \quad 1 \leq i \leq 181, 1 \leq j \leq 22 \quad (5)$$

The Mexican-hat wavelet (Torrence and Compo, 1998) is applied to identify the main oscillations in the composite mean OLR. During the entire 181 days, the major period is about 90 days (Figure 1(a)), which indicates that the seasonal oscillation is the main feature of SCSSM. Day 0 forms the division between positive (suppressed convection) and negative (enhanced convection) wavelet transform coefficients (Figure 1(a)). The seasonal variations (period > 90 days) could explain almost 87% variance of the composite mean OLR.

Table I. The onset date of the South China Sea summer monsoon

Year	Date	Year	Date
1980	14 April	1991	9 June
1981	14 April	1992	20 May
1982	4 June	1993	9 June
1983	25 May	1994	4 May
1984	29 April	1995	14 May
1985	24 April	1996	9 May
1986	14 May	1997	20 May
1987	9 June	1998	25 May
1988	25 May	1999	24 April
1989	20 May	2000	9 May
1990	20 May	2001	9 May

Compared to the seasonal variations, the intraseasonal periods (10–20 days and 30–60 days) are less obvious, especially before onset. Only scattered peaks occur around either the 10–20-day or the 30–60-day period. The normalized reconstructed 90–120-day scale-averaged timeseries shows a shift from a period of suppressed convection before day 0, to one with enhanced convection after the onset.

In order to examine the intraseasonal features, seasonal variations have to be removed. A simple way is to subtract the individual-year value from the composite mean. A wavelet analysis of the OLR anomaly of individual years shows that fluctuations are most energetic at two general periodicities, around 10–20 days and 30–60 days. As an example, the ISOs of the OLR anomaly in 1989 are very obvious at both the 10–20- and the 30–60-day periods (Figure 1(b)). Most of the wavelet-transform coefficients alternating between positive and negative values are around 10–20 days and 30–60 days, and the fluctuations are most energetic after the onset. It seems that two general periodicities around 15 and 45 days are active around the monsoon onset, which are consistent with the results of Mao and Chan (2005). Such a relationship suggests the possibility of using the intraseasonal oscillation signal to investigate the evolution of the SCSSM, which will be considered further in Section 4.

### 3.2. Propagation patterns of the ISO

Previous studies suggest that the ISO exhibits rather different propagations (e.g. Yasunari, 1979, 1981; Krishnamurti and Subrahmanyam, 1982; Chen *et al.*, 1988; Annamalai and Slingo, 2001; Murakami, 1980; Zhu and Wang, 1993). An examination of the variations of the 850-hPa zonal wind before and after the SCSSM onset suggests the 10–20-day mode along the equator to be associated with a slightly westward propagation (Figure 2(a)), while the 30–60-day mode exhibits eastward propagation along the equator (Figure 2(b)). Meanwhile, along the latitude band of the SCS domain, the 850-hPa westerly anomalies of the 10–20-day mode tend to be strong around day –10, and start to be very active at day 0, later break at day 9. The break lasts for around 15 days and active westerly anomalies prevail again over the SCS around day 25 to day 40 (Figure 2(c)). Apart from the 10–20-day mode, activities related to the 30–60-day mode show eastward propagation (Figure 2(d)). Note that the 30–60-day mode of westerly anomalies is pronounced before the SCSSM onset. These enhanced ISO activities (10–20-day and 30–60-day modes) might have a strong relationship with the westerlies' outbreak over the SCS, and such an asynchronous phase between the two modes may be a cause of the monsoon break, and a coupling of 10–20-day and 30–60-day modes could have a direct contribution to the onset and evolution of SCSSM, which will be further examined in Section 4.

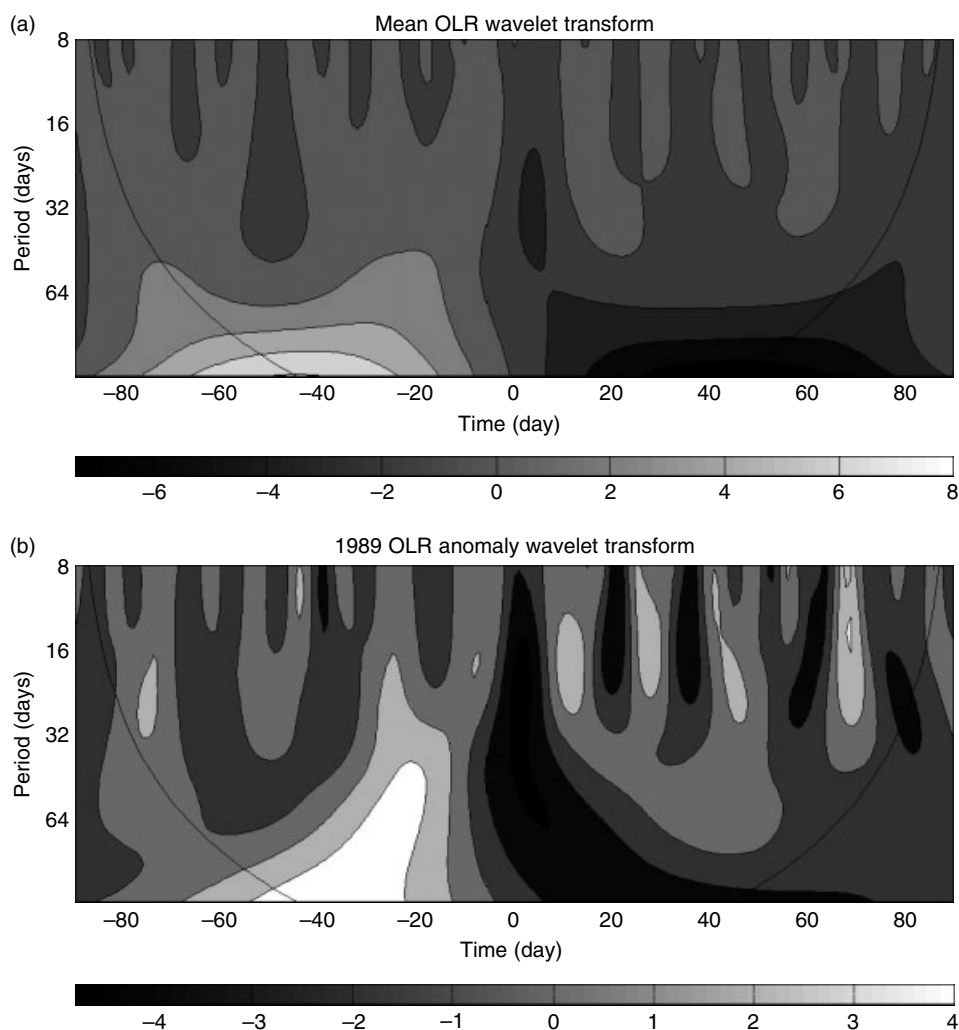


Figure 1. Normalized local wavelet power spectrum of OLR anomaly over SCS: (a) Mean and (b) 1989. Day 0 represent the SCSSM onset day, day (-80) indicates 80 days ahead of onset day, day (80) indicates 80 days after the onset day. The thick curve on either end indicates the edge effects

#### 4. ISO ACTIVITIES IN THE SCSSM EVOLUTION

##### 4.1. The 10–20-day mode

Lagged regression maps of OLR with 850-hPa wind,  $Q_1$ , and  $Q_2$  fields, respectively, for a complete cycle of the 10–20-day mode, from lag -7 to lag 8, are shown in Figures 3–5. One cycle of the 10–20-day band takes about 15 days, with most inactive convection at lag -7 and lag 8, and most active convection at lag 0. The convection and circulation then gradually evolve between these extremes.

At lag -7, the entire SCS domain is dominated by an anticyclonic anomaly (Figure 3) but convection is observed from the Arabian Sea to the Bay of Bengal (BOB), which could be related to the India–Burma trough, from the southern part of China to the East China Sea, and over the western Pacific. Over the East China Sea, a cyclonic circulation appears and becomes organized at lag -6, and becomes prominent to the east of the Philippines by lag -5; meanwhile the anticyclone over the SCS weakens. Accompanying the formation of the Philippine cyclone, convection over the western Pacific develops and moves northwestward. The Philippine cyclone continuously moves westward starting from lag -4; finally at lag 0 a cyclone instead

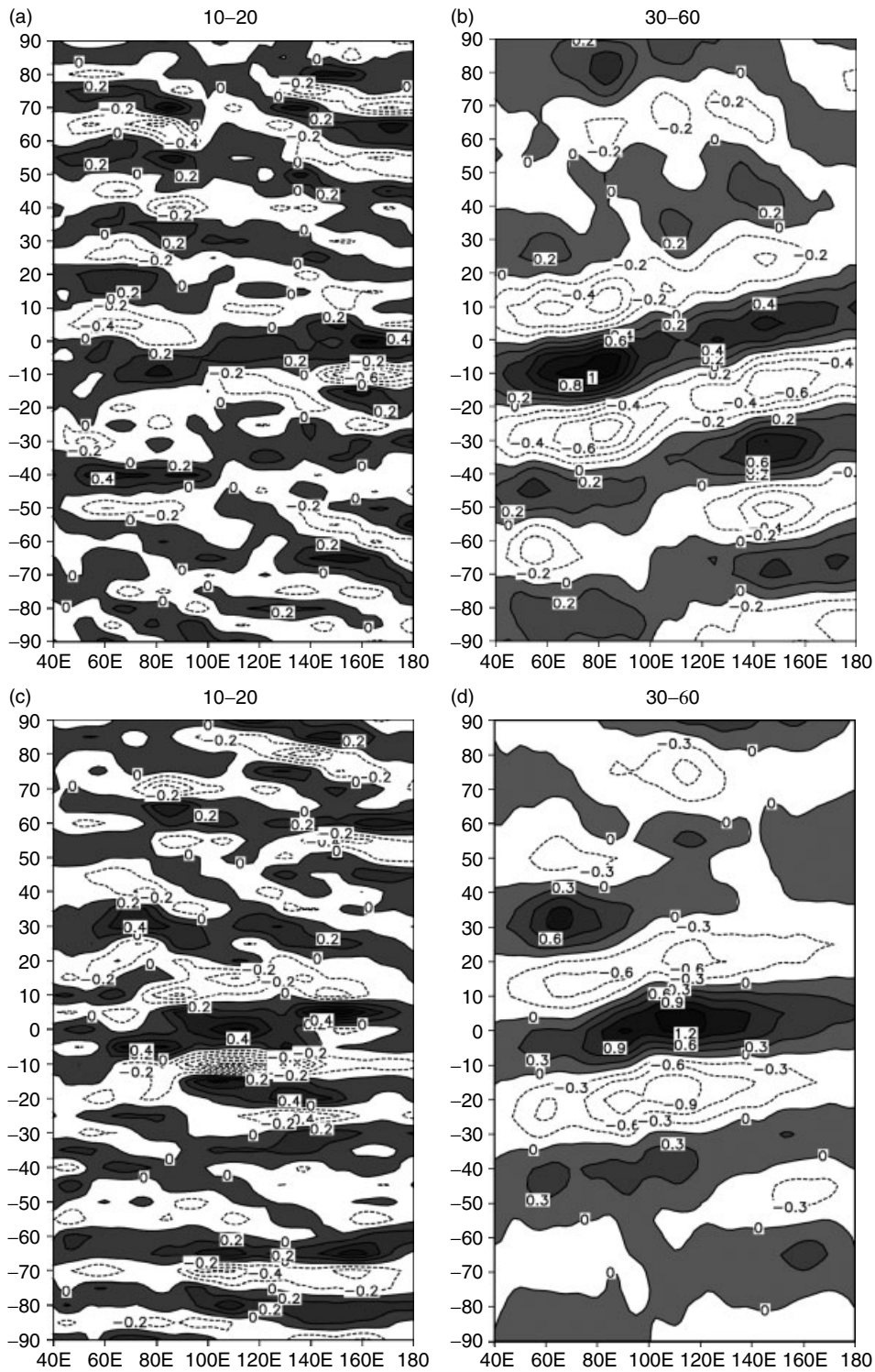


Figure 2. Longitude–time section of 10–20-day and 30–60-day reconstructed composite 850-hPa zonal wind anomalies (unit:  $\text{m s}^{-1}$ ) averaged over ((a) and (b) respectively)  $5^{\circ}\text{S}$ – $5^{\circ}\text{N}$  and [(c) and (d) respectively]  $5^{\circ}$ – $15^{\circ}\text{N}$ . Day 0 represents the onset day,  $-90$  ( $+90$ ) refers to the 90 days before (after) onset date. Shaded areas indicate westerlies

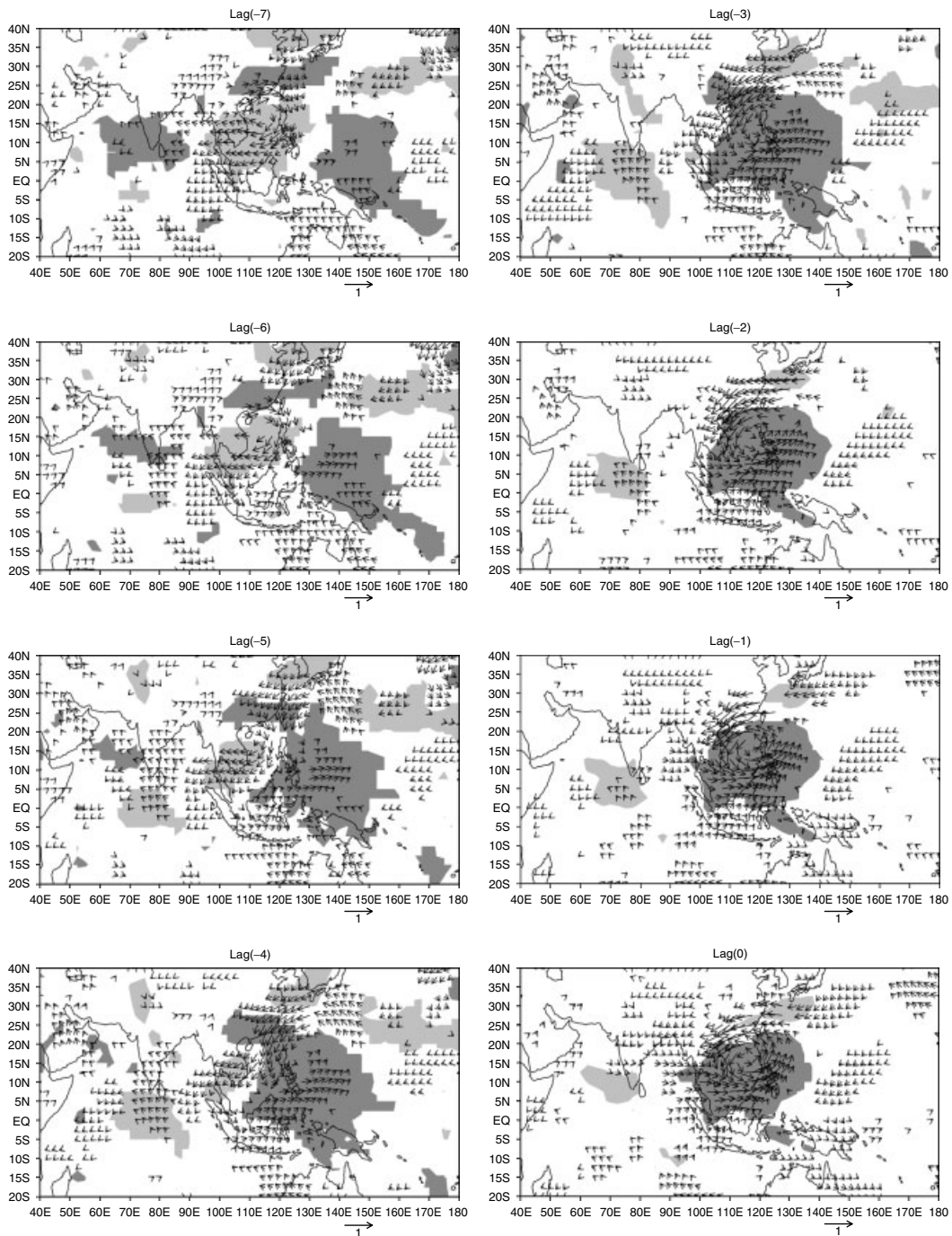


Figure 3. Lagged regression of the 10–20-day filtered OLR (shading, unit:  $W m^{-2}$ ) and 850-hPa wind (arrows, unit:  $m s^{-1}$ ) against the reference OLR. Dark (light) shadings are for  $OLR \leq (\geq) 5.6 W m^{-2}$ , i.e. one half of the standard deviation of the reference OLR. Only values exceeding the 95% significance level have been plotted

of an anticyclone dominates the entire SCS domain. Deep convection occurs then, which might be interpreted as the SCSSM onset. This biweekly disturbance primarily emanates from the equatorial western Pacific (Nitta, 1987) and move northwestward at a rate of 5–6  $m s^{-1}$  prior to the onset.

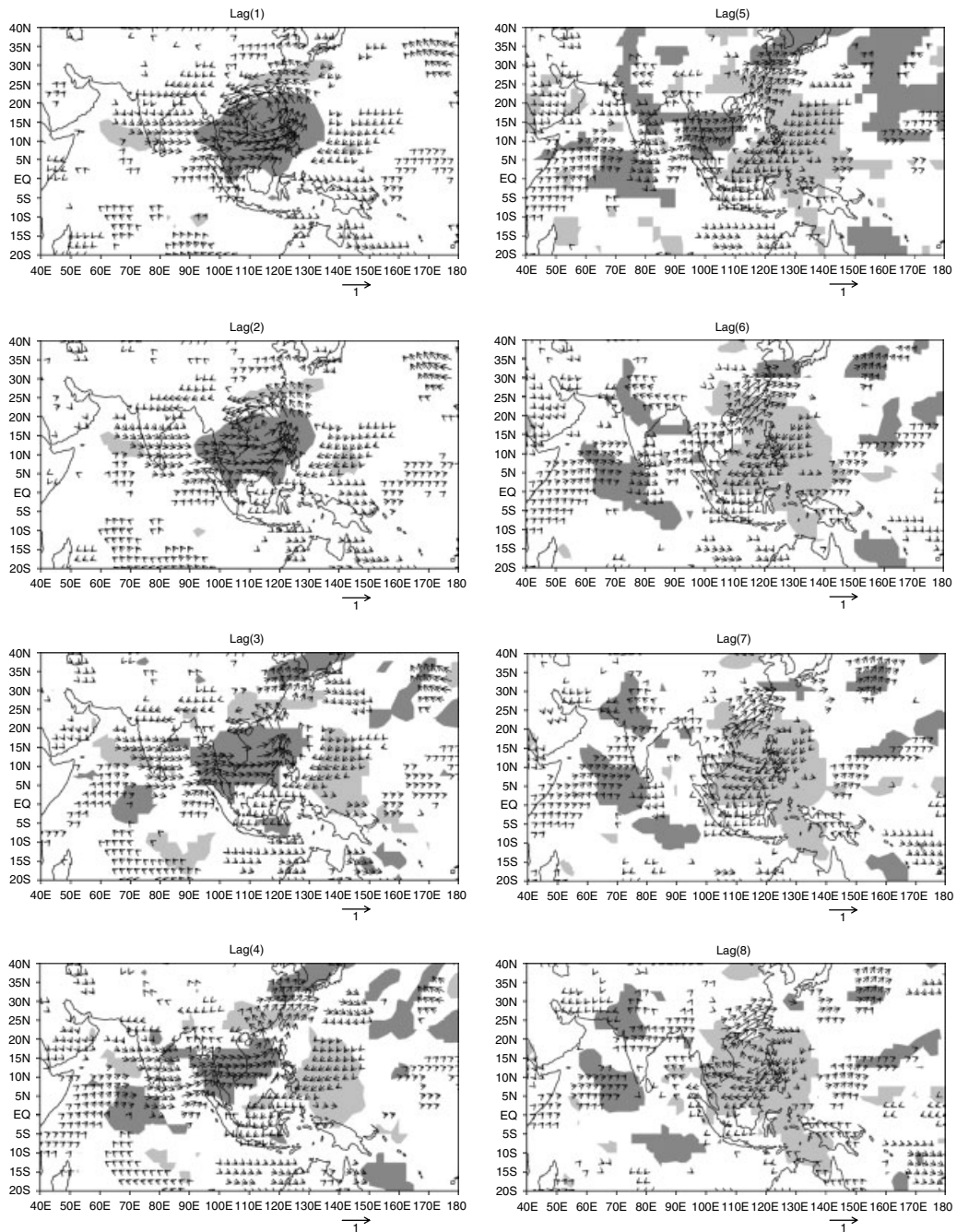


Figure 3. (Continued)

The second half cycle repeats in a reverse way. After onset, this strong cyclone accompanied by significant convection over the SCS remains almost unchanged until lag 4. Meanwhile a weak anticyclonic circulation begins to form to the southeast of Japan at lag 3 and its center moves to the east of the Philippines at lag 5, while the cyclonic circulation over the SCS weakens almost completely at lag 6 because of the continuous expansion of the Philippine anticyclone, and finally an anticyclone prevails over the entire SCS domain at lag 7–8. Convection over the SCS is then suppressed.

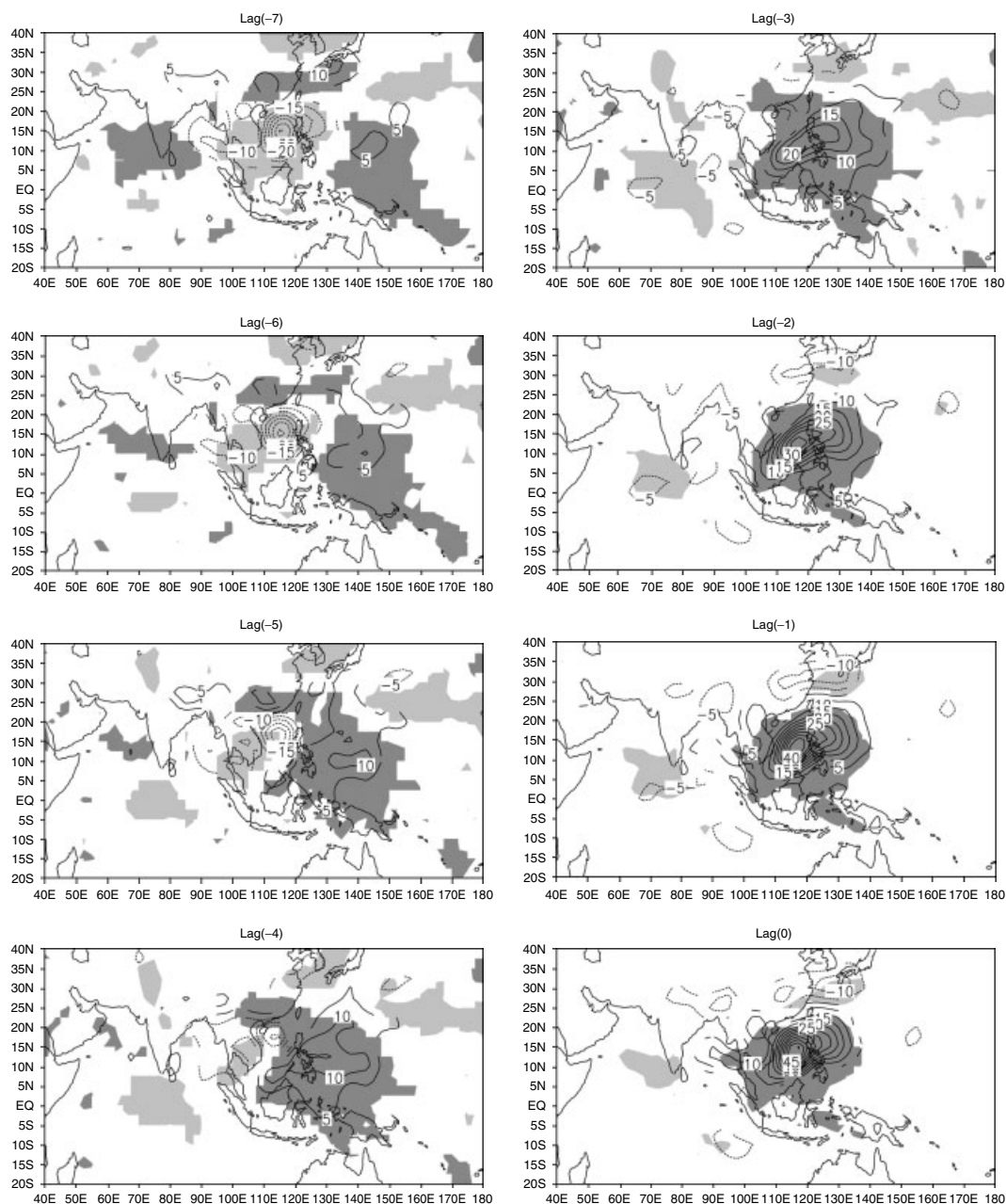


Figure 4. Lagged regression of the 10–20-day filtered OLR (shading, unit:  $\text{W m}^{-2}$ ) and  $Q_1$  (integrated from surface pressure to 100 hPa) (contour, unit:  $\text{W m}^{-2}$ ) against the reference OLR. Dark (light) shadings are for OLR  $\leq$  ( $\geq$ )  $5.6 \text{ W m}^{-2}$ , i.e. one half of the standard deviation of the reference OLR. Only values exceeding the 95% significance level have been plotted

The northwestward propagation of the 10–20-day band prior to the SCSSM onset highlights the role of the convection over the equatorial western Pacific, where the off-equatorial ITCZ emanates, in the intraseasonal variation of the SCSSM. However, for the break of the SCSSM, the contribution of the 10–20-day mode appears to come from the mid-latitudes. Since the focus here is on the conditions prior to the SCSSM, this latter part will not be explored further. For more details of how the ISO modulates the monsoon active/break cycle, the reader is referred to the recent studies of Chan *et al.* (2002) and Mao and Chan (2005).

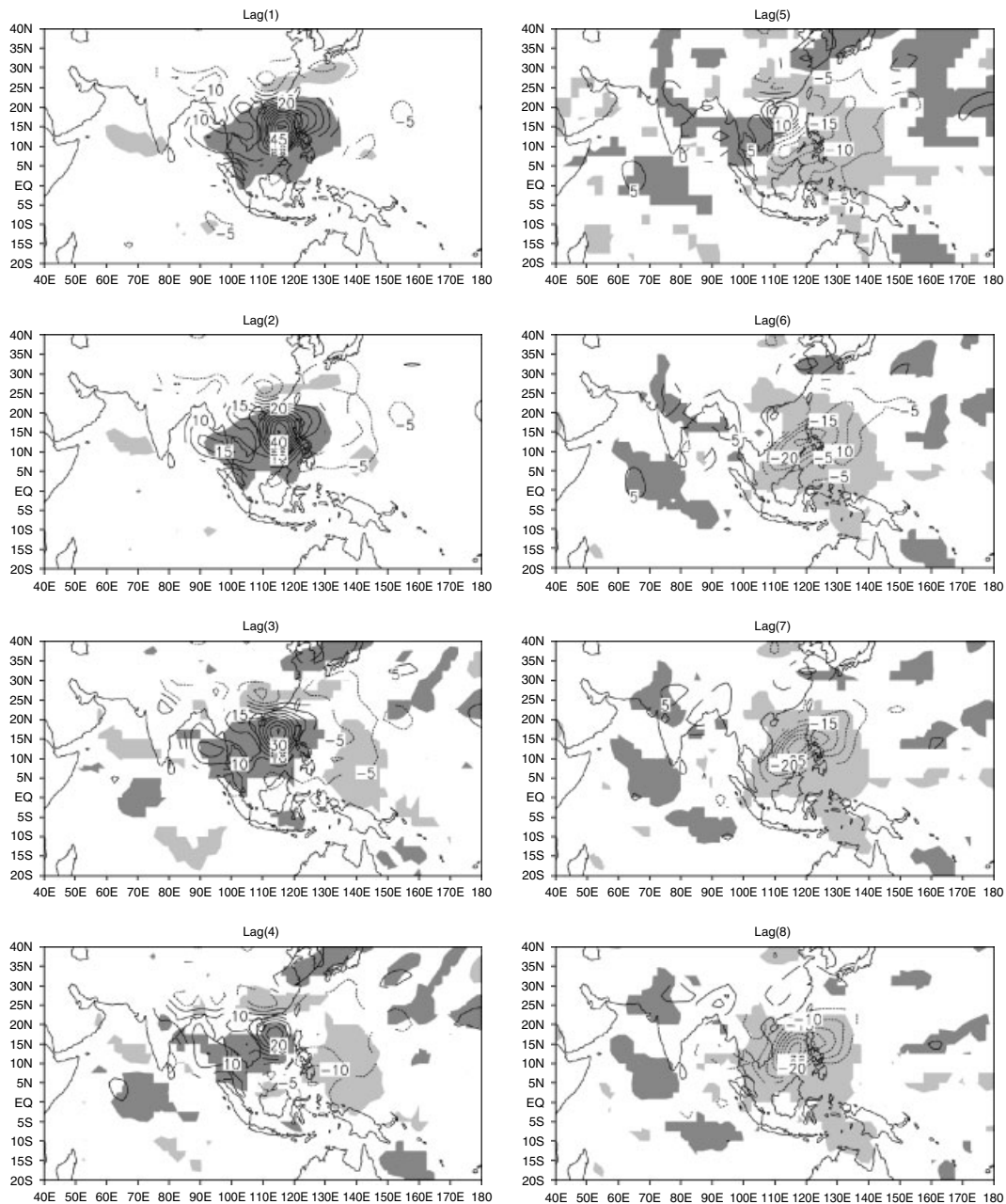


Figure 4. (Continued)

Consistent with the circulation, a lagged regression map of  $Q_1$  ( $Q_2$ ) against OLR shows a similar propagation of the 10–20-day mode, as shown in Figure 4 (Figure 5). At lag  $-7$ , negative values of  $Q_1$  and  $Q_2$  over the SCS are found, which suggests evaporation exceeding precipitation (Figures 4–5), while positive values are observed over the East China Sea, indicating intensive convection. At lag  $-6$ , positive values of  $Q_1$  and  $Q_2$  appear over the western Pacific and generally increase at lag  $-5$ . Furthermore, a systematic westward movement of the maximum  $Q_1$  and  $Q_2$  accompanies the Philippine cyclone (Figure 3) from lag  $-4$  to lag 0. These characteristics suggest an influence on the moisture source of the SCSSM. The time of occurrence of the peaks in the  $Q_1$  and  $Q_2$  fields corresponds well to each other as well as to the

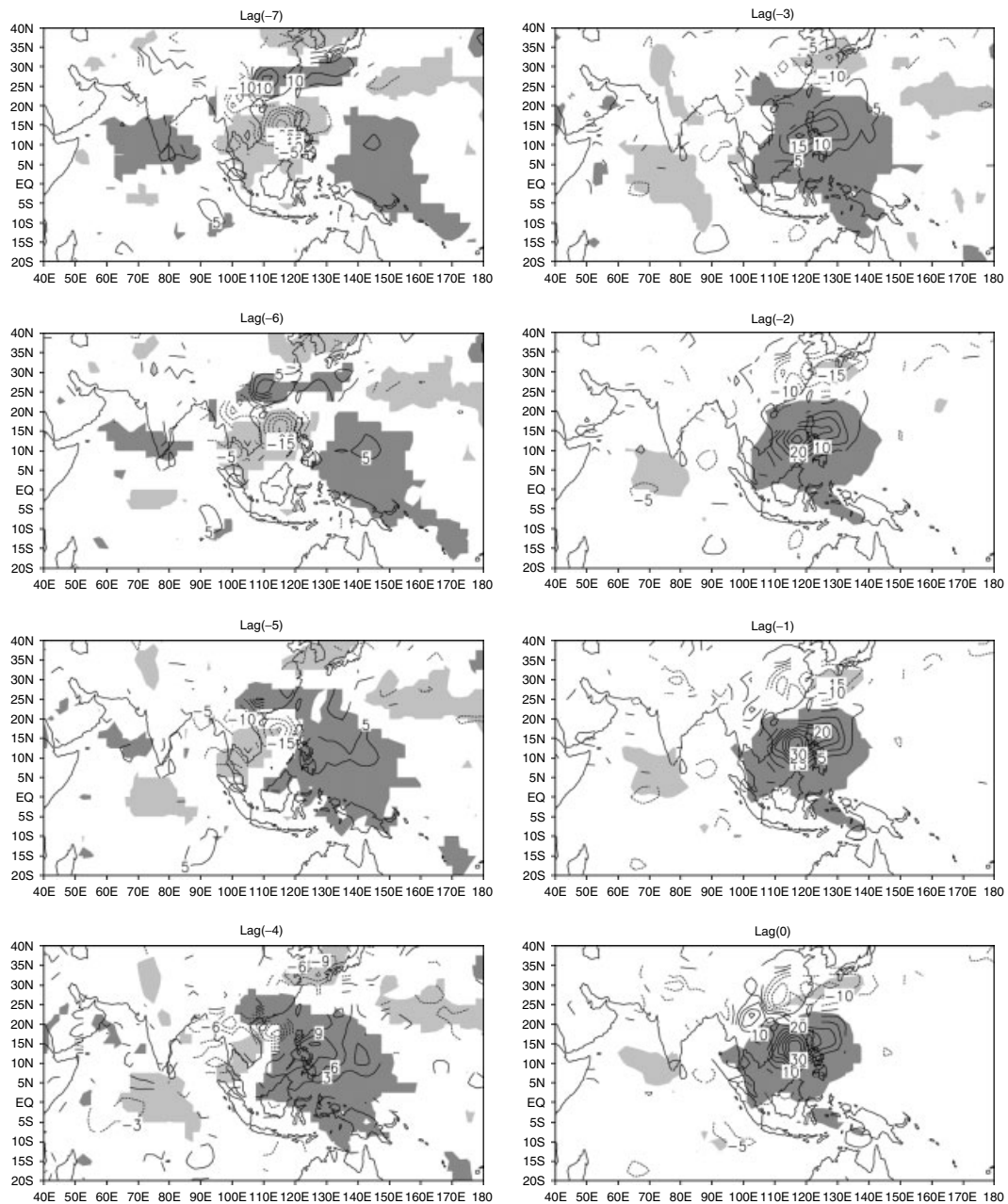


Figure 5. Lagged regression of the 10–20-day filtered OLR (shading, unit:  $\text{W m}^{-2}$ ) and  $Q_2$  (integrated from surface pressure to 100 hPa) (contour, unit:  $\text{W m}^{-2}$ ) against the reference OLR. Dark (light) shadings are for  $OLR \leq (\geq) 5.6 \text{ W m}^{-2}$ , i.e. one half of the standard deviation of the reference OLR. Only values exceeding the 95% significance level have been plotted

cyclonic anomalies in the circulation (Figure 3), which indicates contributions from the released latent heat of condensation. Then a subtropical anticyclone in the lower troposphere is formed to the east of the deep convective condensation heating (Wu *et al.*, 1999b; Liu *et al.*, 2001; Rodwell and Hoskins, 2001).

Around the SCSSM onset, appreciable moisture appears to come into the SCS from the equatorial western Pacific because of the southerly to the west of such an induced subtropical anticyclone, which contributes to the development of convection and condensation heating there (Liu *et al.*, 2002). So the entire SCS region

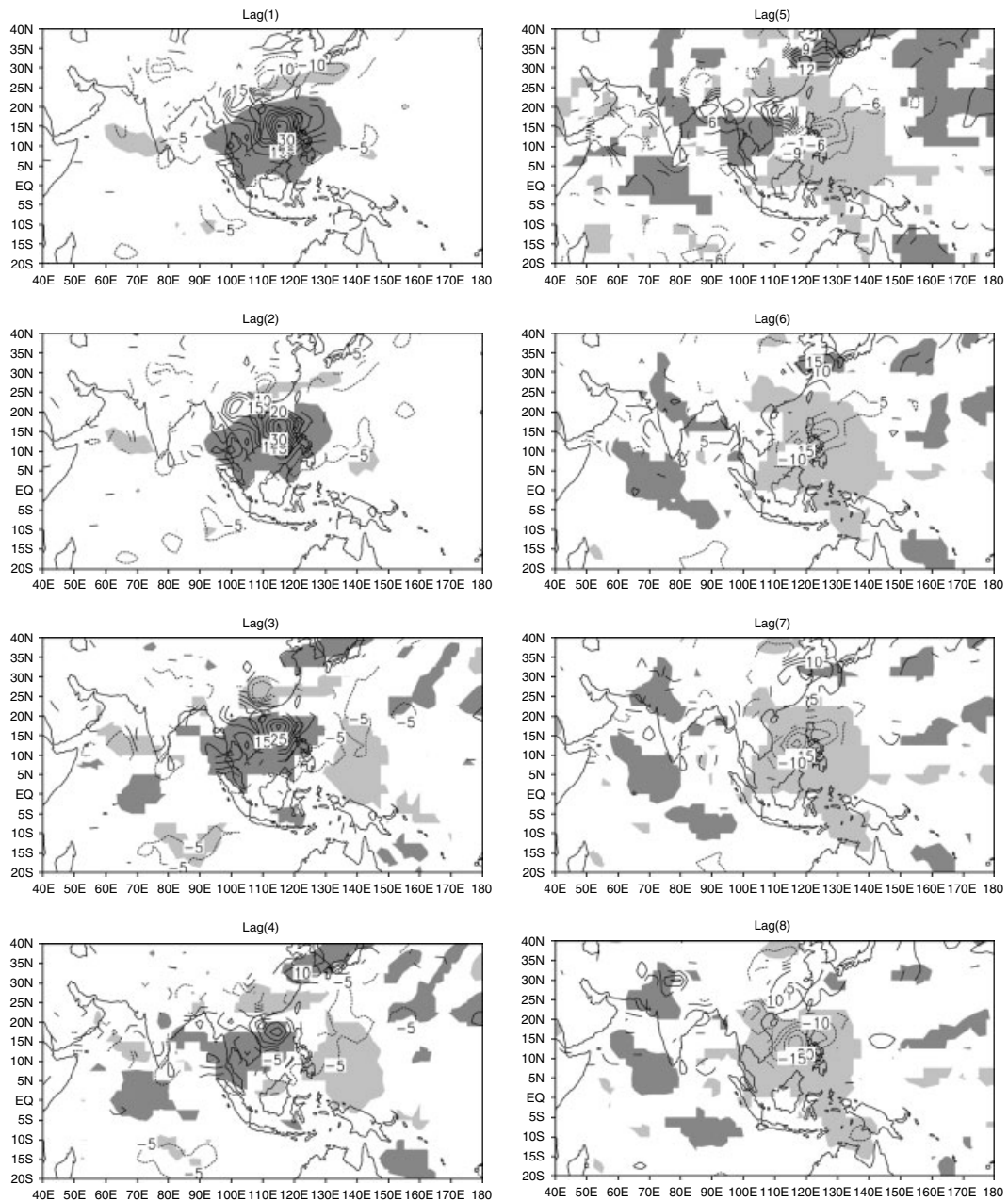


Figure 5. (Continued)

becomes an obvious water vapor sink. Deep convection then becomes the strongest, because strongest  $Q_1$  and  $Q_2$  occur at lag 0. SCSSM onset will then be triggered and the subtropical anticyclone will appear weakened. Afterwards, the deep convection starts to weaken by the continuous evaporation of water vapor from lag 4 and finally negative values of  $Q_1$  and  $Q_2$  appear at lag 7–8 because an anticyclone originally formed to the east of the deep Philippine convective condensation heating (Wu *et al.*, 1999b; Liu *et al.*, 2001; Rodwell and Hoskins, 2001) prevails again over the entire SCS domain (Figure 3).

In terms of the 10–20-day oscillation, it appears that the western Pacific subtropical high (WPSH) has been weakened and separated into two parts because of the cyclone over the East China Sea, with one anticyclone

remaining over the SCS domain, the main part of WPSH still prevailing over the western North Pacific. The former probably contributes to the strong evaporation (negative  $Q_2$ ) and obvious cooling (negative  $Q_1$ ) over the SCS domain 8 days prior to the SCSSM onset, and the convection there is therefore suppressed. Meanwhile, weak convection is observed over the BOB region, the East China Sea and the western Pacific, with weak water vapor sink and little latent heat release. But over the western Pacific, there exists strong latent-heat release. This area of maximum  $Q_1$  propagates northwestward 6 days before the onset, while the other two water-vapor sinks over the BOB and East China Sea diminish. Then 2 days later, a cyclonic circulation over the East China Sea becomes organized and migrates to the east of the Philippine Sea. As a result, the convection over the southern part of China merges with the enhanced convection from the western Pacific. On the other hand, the water-vapor sink over the BOB disappears when the SCS anticyclone weakens and moves westward, so the convection is suppressed as a result of the BOB trough being replaced by a weak ridge. Thus prediction on the establishment and development of the SCSSM should consider the influence of the 10–20-day mode. More explanation will be given in section 4.3 in terms of the physical meaning and evidence of the 30–60-day mode, which will be discussed in following subsection.

#### 4.2. The 30–60-day mode

A complete cycle of the 30–60-day mode is about 45 days. The convection is most suppressed over SCS domain at lag  $-21$  or lag  $24$ , and strongly enhanced at lag  $0$ .

From the circulation point of view, at lag  $-21$ , the SCS domain is dominated by an anticyclone (Figure 6), and one of several discrete convective centers develops over the southern Indian Ocean and extends northeastward. The convection or monsoon trough continues to move from the equatorial Indian Ocean (at lag  $-18$ ) to the BOB (at lag  $-12$ ), but the SCS anticyclone still prevails before lag  $-18$ , and then weakens gradually starting from lag  $-15$ . Meanwhile, convection evolves into a large band along the equator and this monsoon trough propagates northward from  $5^\circ\text{N}$  at lag  $-12$ , to  $10^\circ\text{N}$  at lag  $-9$ ,  $15^\circ\text{N}$  at lag  $-3$ , and finally dominates the entire SCS domain. It is noted that preceding the SCSSM onset, the monsoon trough at BOB moves eastward, and meets with a cyclonic circulation to the east of the Philippines so that a cyclone instead of the anticyclone prevails over the SCS domain at lag  $0$ .

After the onset, to the south of this convection belt centered over the SCS, an anomalous anticyclonic flow develops over the Indian Ocean and the BOB region at lag  $3$ , and covers the tropics from the Indian Ocean to the western Pacific at lag  $9$ . Meanwhile, the convection and anomalous westerlies over the SCS weakens significantly by lag  $12$ . The anticyclonic circulation over the BOB moves into the SCS slowly at lag  $15$  so that an anticyclone dominates much of the SCS, and finally the whole SCS and the Philippine Sea at lag  $24$  so that convection is suppressed. Thus, it takes 24 days to change the SCS cyclone into an anticyclone again.

Chen and Chen (1995) suggested that the low-level 30–60-day mode is associated with a kind of monsoon trough and ridge in the 1979 summer monsoon over the SCS region. The current result is therefore consistent with that from their case study. Notice also that deep convection begins to develop along the equatorial area. In addition, the monsoon trough is well developed, with enhanced convection in a band extending from the Indian Ocean to the western Pacific. Thus, an obvious cyclonic–anticyclonic–cyclonic circulation pattern is set up from the equator to the north together with the alternating strong–weak–strong convection belts. This pattern is very similar to the situation for the SCS monsoon-active and break phase illustrated by Mao and Chan (2005).

Such a flow pattern migrates initially eastward then northward so that the anticyclone over the SCS weakens and convection over the SCS is significantly enhanced. The most prominent feature is the so-called trough–ridge seesaw in which the monsoon trough and ridge exist alternatively over the SCS, enhancing or suppressing the convection. Such a seesaw phenomenon applies not only for the monsoon onset/end cycle but the monsoon active/break cycle, suggesting the interactions between the tropics and extratropics on a 30–60-day timescale.

A lagged regression map of  $Q_1$  ( $Q_2$ ) against OLR shows a similar propagation of the 30–60-day mode, as shown in Figure 7 (Figure 8). At lag  $-21$ , negative values (evaporation) of  $Q_1$  and  $Q_2$  over the SCS are found to be similar to those at lag  $-7$  of the 10–20-day mode, but positive values (condensation) are scattered

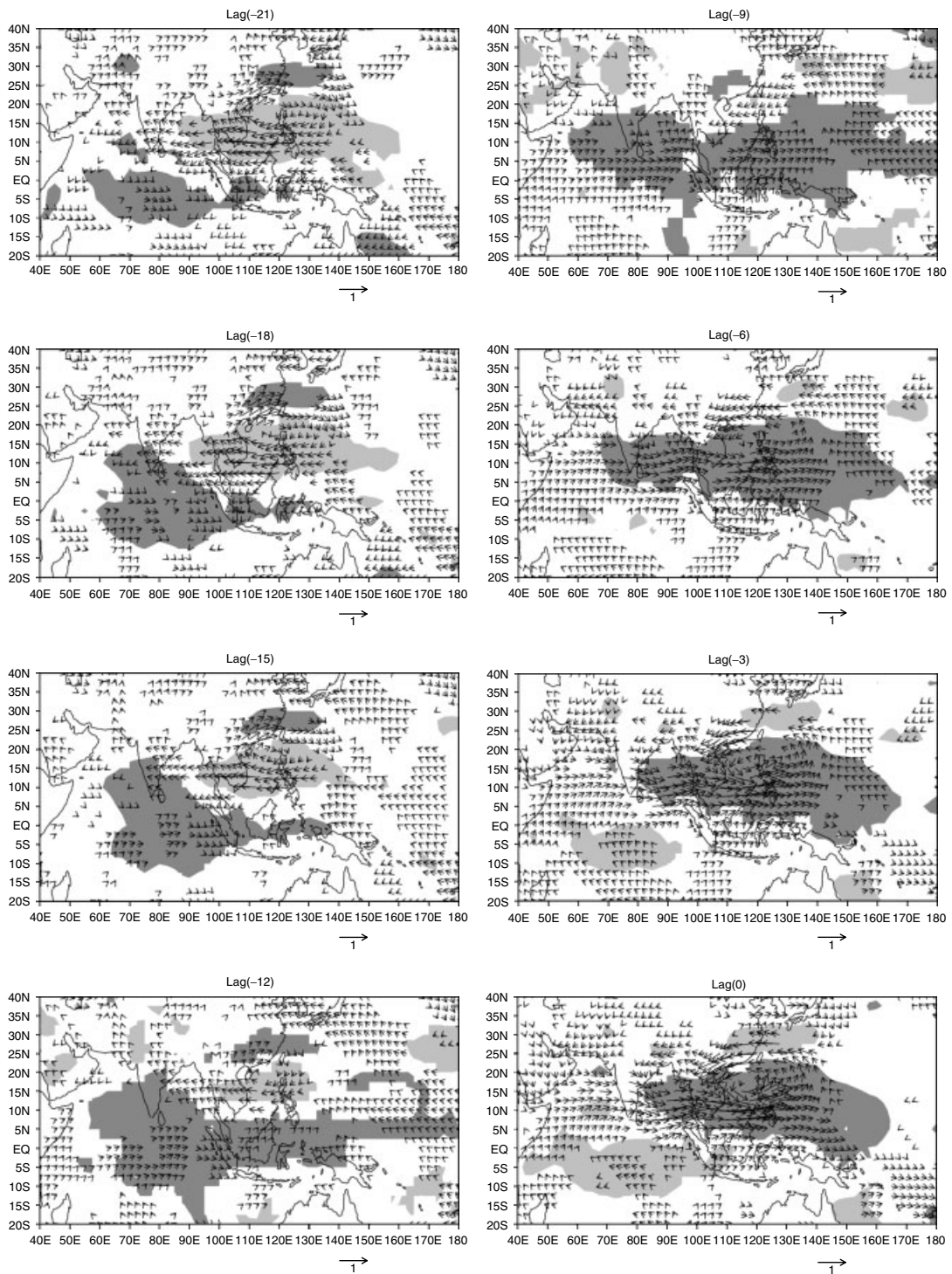


Figure 6. Lagged regression of the 30–60-day filtered OLR (shading, unit:  $W m^{-2}$ ) and 850-hPa wind (arrows, unit:  $m s^{-1}$ ) against the reference OLR. Dark (light) shadings are for  $OLR \leq (\geq) 3.3 W m^{-2}$ , i.e. one half of the standard deviation of the reference OLR. Only values exceeding the 95% significance level have been plotted

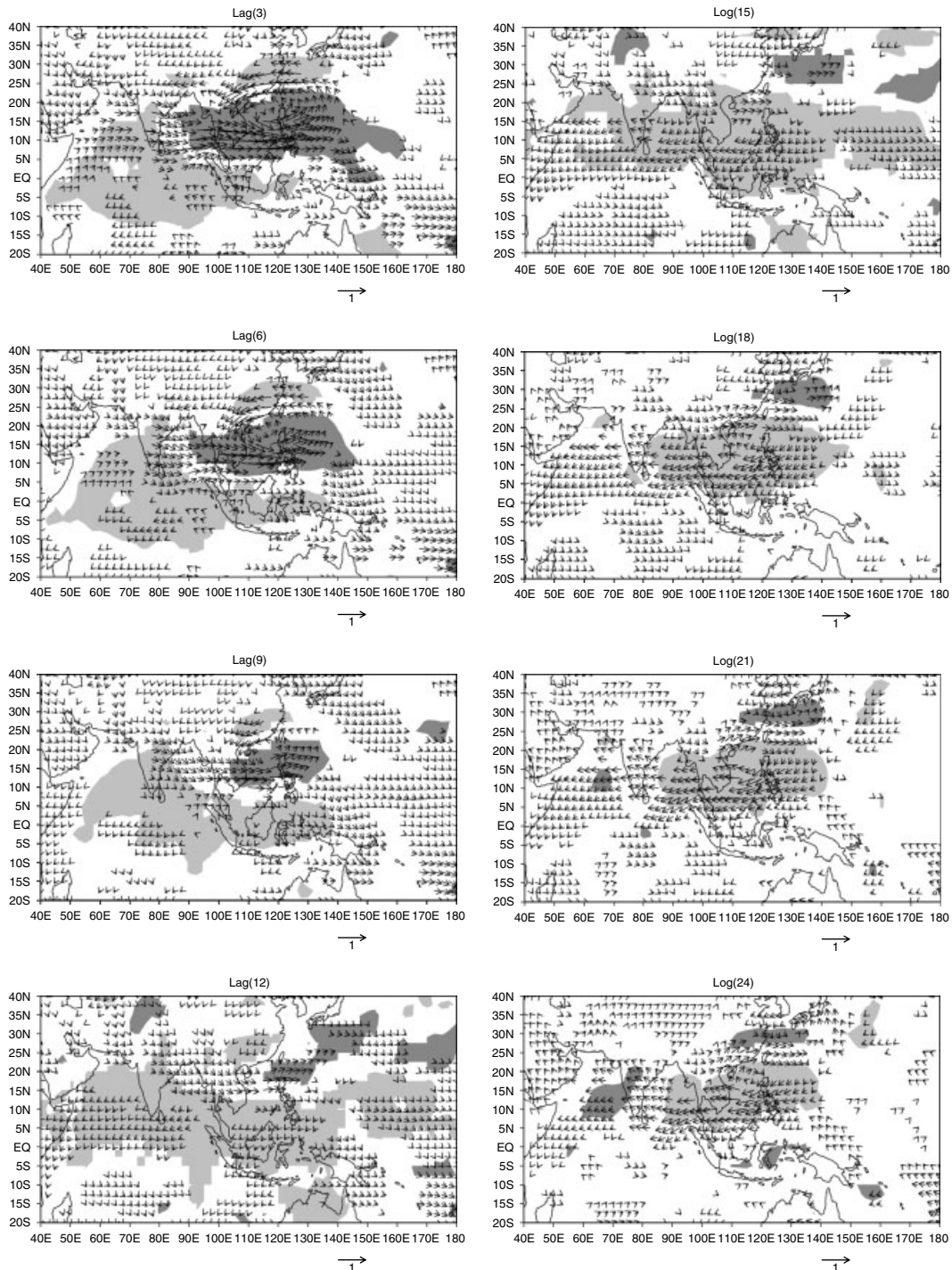


Figure 6. (Continued)

over the East China Sea and the Indian Ocean. Obviously, the positive values of  $Q_1$  and  $Q_2$  over the Indian Ocean increase and extend into a larger band along the equator at lag  $-12$ , and then this large band—the off-equatorial ITCZ or the monsoon trough—systematically move northward (lag  $-6$ ), finally reaching the

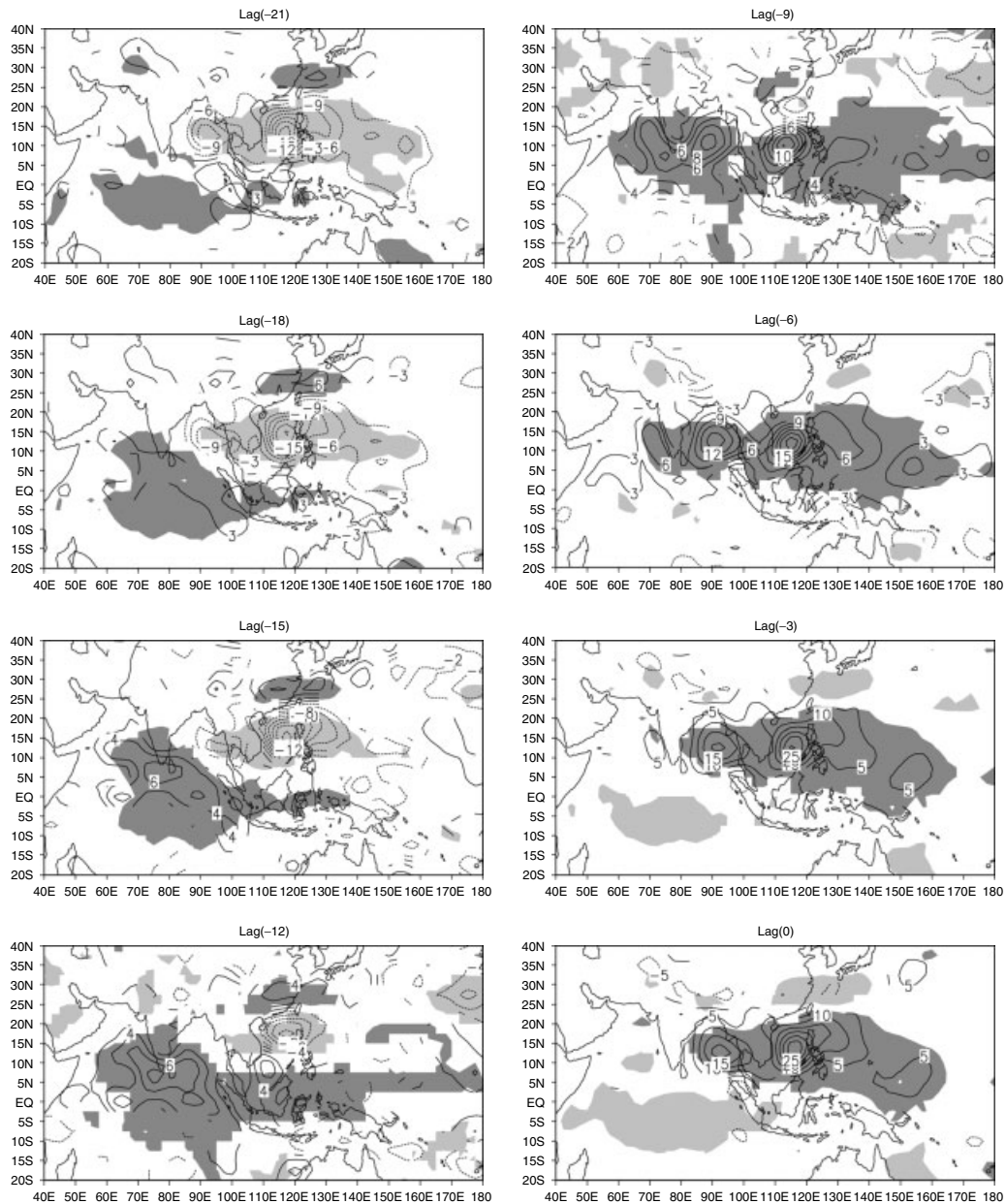


Figure 7. Lagged regression of the 30–60-day filtered OLR (shading, unit:  $\text{W m}^{-2}$ ) and  $Q_1$  (integrated from surface pressure to 100 hPa) (contour, unit:  $\text{W m}^{-2}$ ) against the reference OLR. Dark (light) shadings are for  $OLR \leq (\geq) 3.3 \text{ W m}^{-2}$ , i.e. one half of the standard deviation of the reference OLR. Only values exceeding the 95% significance level have been plotted

SCS domain (lag  $-3$  and lag  $0$ ). In general, it takes 21 days for the moisture from the Indian Ocean to reach the SCS.

After the onset, convection over the SCS starts to weaken at lag 3 and the range of the convection shrinks obviously at lag 9 and lag 12, and negative values of  $Q_1$  and  $Q_2$  are located to the southern part of the SCS at lag 12. Furthermore, negative values of  $Q_1$  and  $Q_2$  cover the entire SCS domain at lag 15 and lag 18 with the minimum at lag 24, suggesting that strong evaporation occurs, and the convection is being suppressed again (Figures 7 and 8).

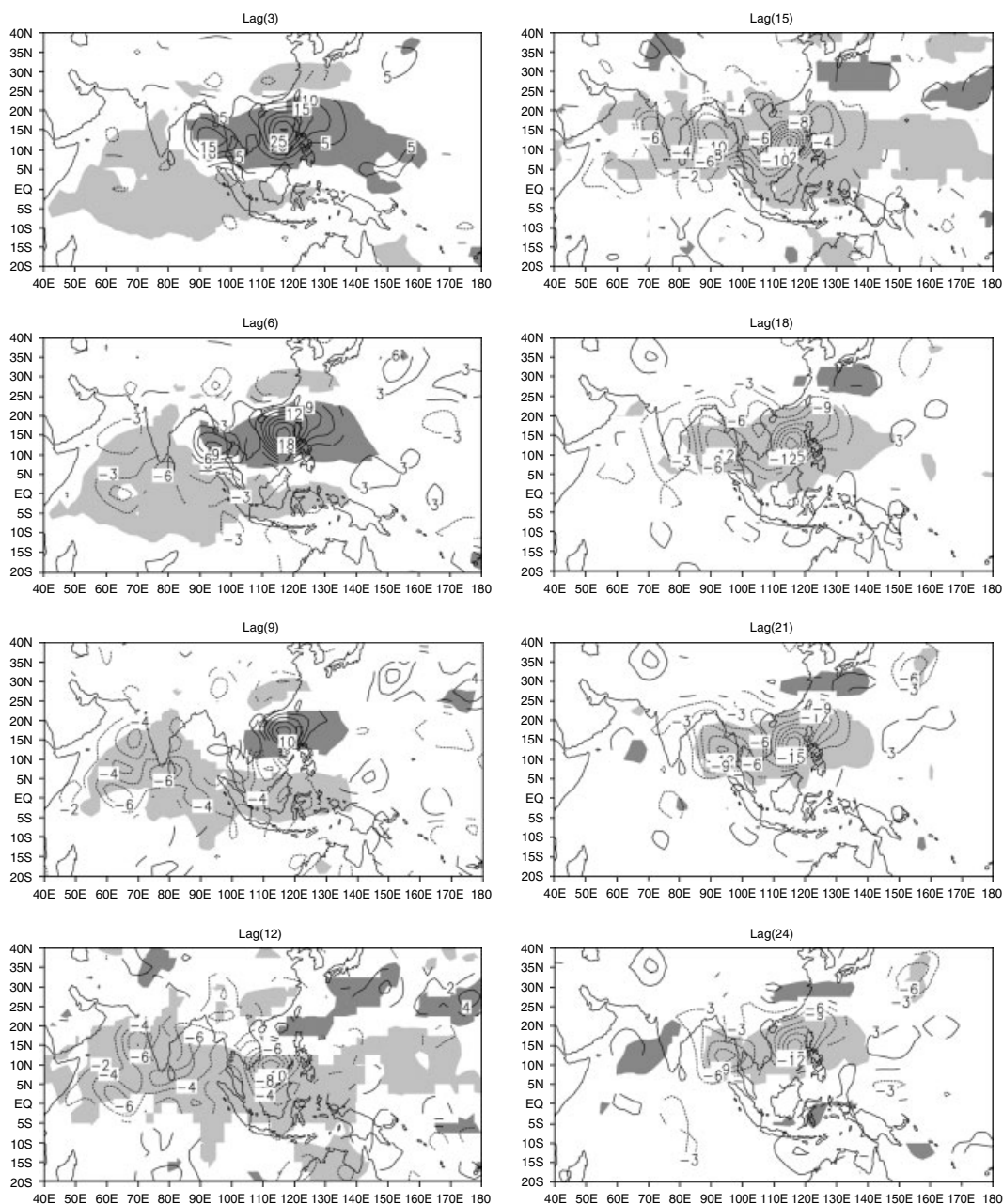


Figure 7. (Continued)

The circulation features described in Figure 6 fit well with the distributions of  $Q_1$  and  $Q_2$ . Twenty-one days prior to the SCSSM onset, the convection over the SCS is suppressed with a moisture source (Figure 8), so that cooling instead of heating occurs over the SCS (Figure 7). One important feature is that the monsoon trough that apparently originates from the equatorial Indian Ocean propagates northeastward, with a developing convective band releasing latent heat at lag  $-9$ . On the contrary, evaporation over the SCS wanes because of the weakening of the anticyclone, and then the monsoon trough penetrates into the southern part of the SCS. From lag  $-6$  to lag  $0$ , this convective band moves continuously northeastward and the entire SCS becomes a water-vapor sink with a cyclone replacement, reaching a peak at lag  $0$ . Afterwards, the latter half cycle

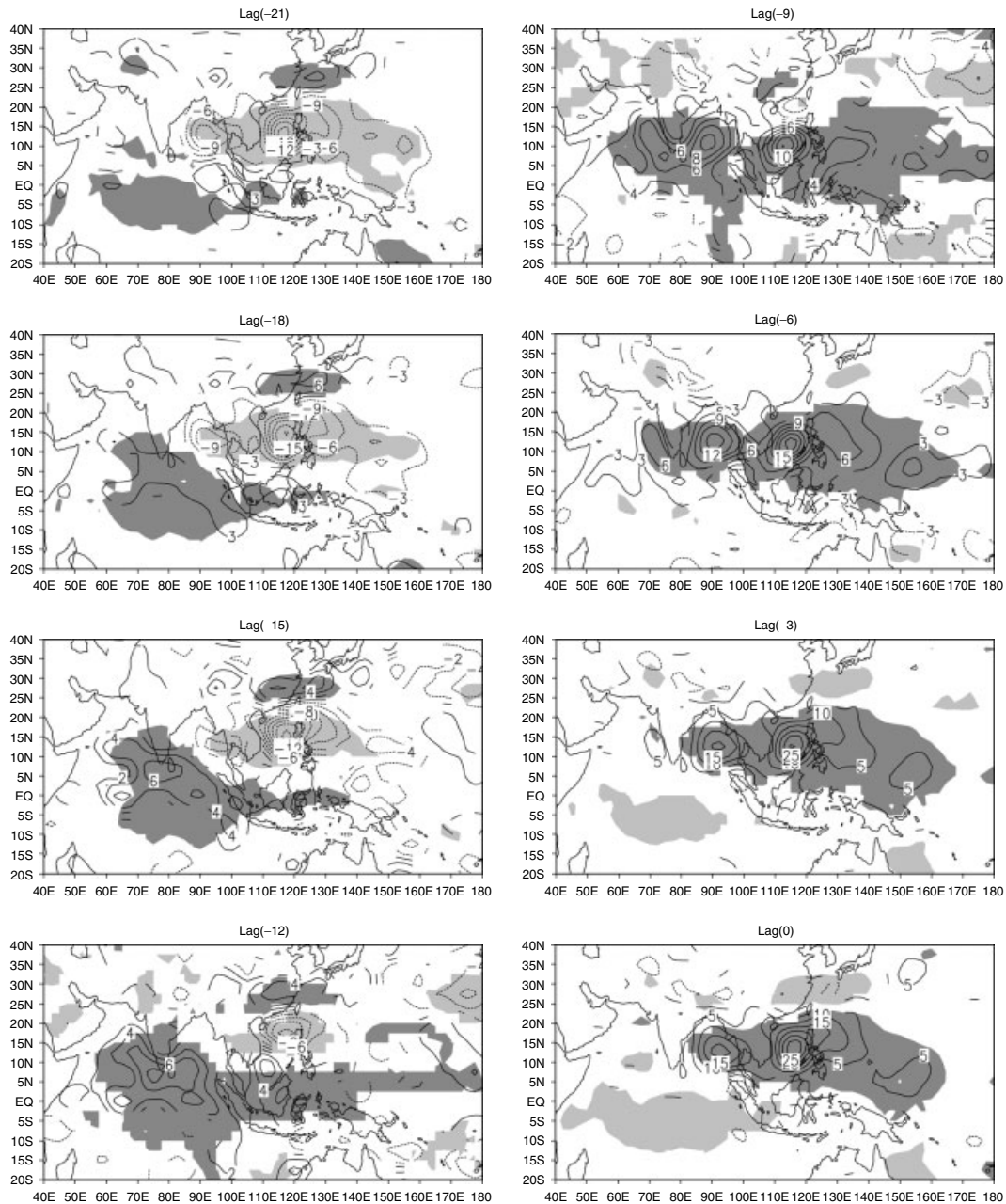


Figure 8. Lagged regression of the 30–60-day filtered OLR (shading, unit:  $\text{W m}^{-2}$ ) and  $Q_2$  (integrated from surface pressure to 100 hPa) (contour, unit:  $\text{W m}^{-2}$ ) against the reference OLR. Dark (light) shadings are for OLR  $\leq$  ( $\geq$ )  $3.3 \text{ W m}^{-2}$ , i.e. one half of the standard deviation of the reference OLR. Only values exceeding the 95% significance level have been plotted

from lag 0 to lag 24 repeats in a reverse way. The band of suppressed convection gradually strengthens and extends eastward until it dominates the entire SCS domain.

The physical processes associated with the 30–60-day mode in relation to the SCSSM onset, therefore, differ from those of the 10–20-day mode. The effect apparently comes from the tropics over the Indian Ocean throughout the cycle. No obvious contribution comes from the mid-latitudes or the equatorial western Pacific.

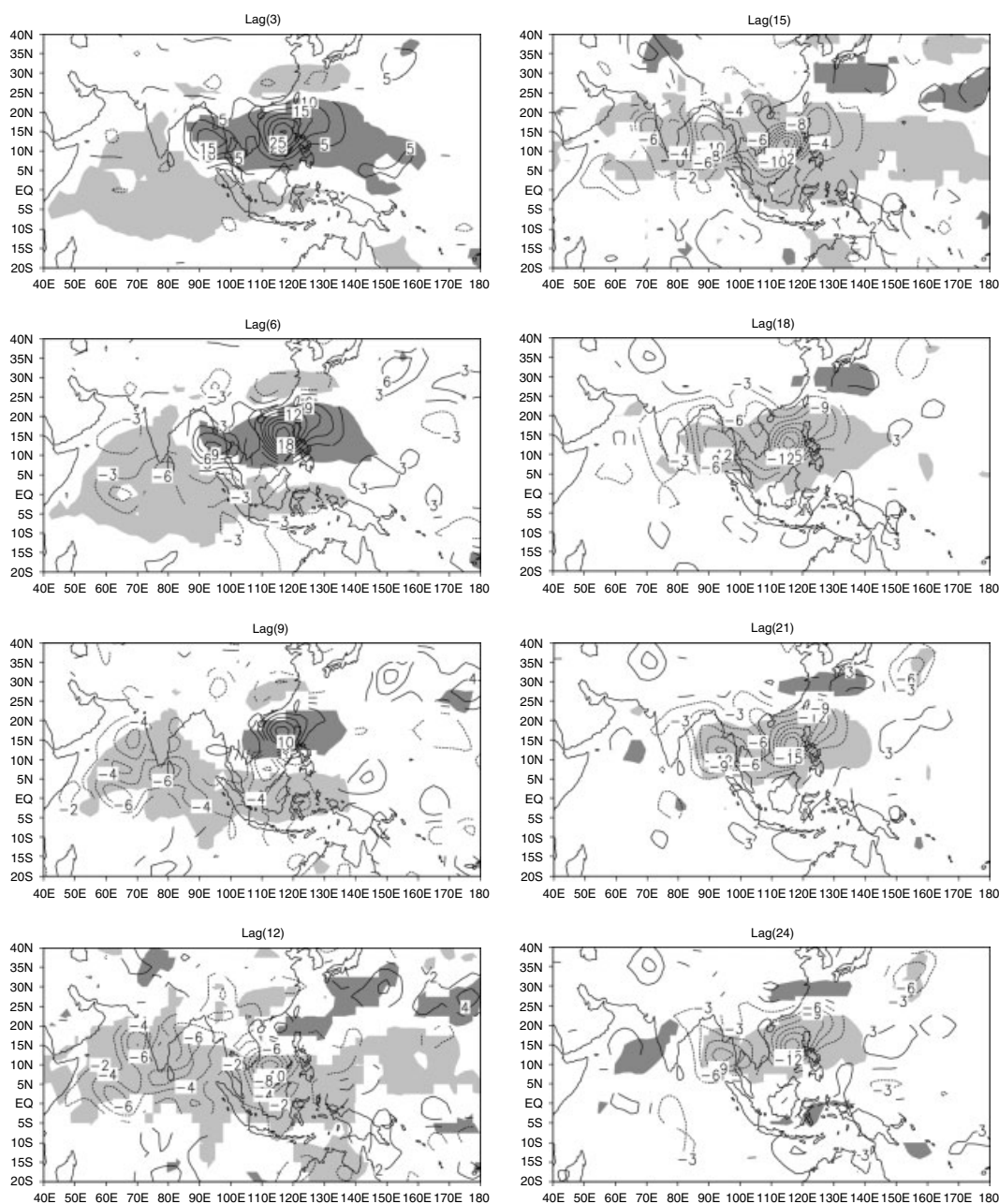


Figure 8. (Continued)

#### 4.3. The role of the ISO

Previous studies (e.g. Chen *et al.*, 1988) have shown that water vapor is transported eastward from the Indian Ocean and northeastward by the western branch of the subtropical high to the SCS. The moisture convergence over the SCS should therefore have a direct contribution to the SCSSM onset.

This aspect is evaluated in the last two sections: SCSSM onset refers to the active period at lag 0 for both modes, and inactive period (monsoon break) at lag 8 (lag 24) in the 10–20-day (30–60-day) mode. The anticyclone over the SCS at lag –7 or lag 8 (lag –21 or lag 24) is consistent with the location of the WPSH.

Before the SCSSM onset, the WPSH dominates over the SCS so that moisture could not flow into the SCS. Around the onset (lag 0), the part of the WPSH over the SCS is replaced by a cyclone, so that westerlies prevail over the SCS. The westerlies are apparently responsible for providing the moisture source for the convection, as has been discussed by Chen *et al.* (1988) and Chan *et al.* (2002). It is interesting to note that the 10–20-day mode is closely associated with the successive northwestward propagation of the active/inactive convection from the equatorial western Pacific, which may have resulted from a Rossby wave response to deep convection originating from the equatorial western Pacific. On the other hand, the 30–60-day mode is largely related with the successive eastward intrusion of the equatorial band of enhanced/suppressed convection from the Indian Ocean. Such a difference in propagation between the two modes indeed reflects their characteristics. It appears that the northwestward propagation mode of the 10–20-day band and the northeastward propagation mode of 30–60-day band may be a mechanism to link with the monsoon evolution in moistening the atmosphere over the SCS as far as the onset is concerned.

Chen and Chen (1993) suggested that the northward-migrating monsoon trough of the 30–60-day mode is a possible mechanism responsible for the development of the low in the Northern Hemisphere of the double-cell structure of the 10–20-day mode and its northward propagation. As can be seen from Figures 4 and 7, the convection over the equatorial western Pacific of the 10–20-day mode migrates northward concomitantly with the 30–60-day monsoon trough or off-equatorial ITCZ, which might also indicate that the northeastward-propagating monsoon trough of the 30–60-day mode initiates the development of the disturbance over the equatorial western Pacific of the 10–20-day mode. Thus, both the 10–20-day and 30–60-day modes are of importance to the SCSSM onset. It appears that the initiation of the 10–20-day convection over the western Pacific may be induced by the 30–60-day monsoon trough over the equatorial Indian Ocean when this convection band extends into the western Pacific, and the coupling between these two modes would result in the SCSSM onset when they reach over the SCS region. The close relation between the ISO and SCSSM onset leads to the following hypothesis.

Prior to the SCSSM onset, westerlies are confined to around the equatorial region (western Pacific and Indian Ocean). Then, deep convection is initiated over the equatorial Indian Ocean and propagates eastward. The westerlies associated with the deep convection migrating to the BOB apparently provide a conduit for the transport of moisture toward the northern part of the SCS (Liu *et al.*, 2002), and result in warm and moist advection over the SCS, which destabilizes the subtropical ridge. Moist westerlies can then penetrate the central and southern part of SCS, bringing heat and moisture to the entire SCS. As shown in Figures 6–8, this process might take 21 days. Meanwhile, probably 7 days preceding the onset date (10–20-day mode) (Figures 3–5), the WPSH dominates over the SCS, and the low-level westerlies cannot penetrate the SCS, so that convection over the SCS is suppressed. But the off-equatorial ITCZ over the equatorial western Pacific is active, which is likely a Rossby wave response to the convection in the ITCZ over the equatorial western Pacific. Furthermore, this continuous northwestward propagation might be related to the 30–60-day monsoon trough, and the lower-level westerlies penetrate the SCS when the WPSH weakens. Consequently, the moisture coming from the cross-equatorial flow originating from the equatorial Indian Ocean and the southwestern flank of the WPSH converge into the SCS then shift to the South China and the eastern China region. Without the aid of two modes, the subtropical ridge will persist over the SCS and SCSSM might not be initiated.

After the SCSSM onset, the behavior of the WPSH is still affected by the latter half cycle of two modes. The WPSH ridge occasionally extending toward the SCS region probably results from an out-of-phase of the two modes, which causes the monsoon break. More details about the active/break cycle of SCSSM have been discussed in Mao and Chan (2005).

## 5. THE SCS ISO DURING ENSO EVENTS

How ENSO interacts with the ISO has been controversial. Some have suggested that strong MJO or ISO activities are associated with the warm ENSO event (e.g. Kessler and McPhaden, 1995; McPhaden, 1999; Xu and Chan, 2001), while others showed the opposite result that MJO activities have no significant relationship

with ENSO (e.g. Hendon *et al.*, 1999; Slingo *et al.*, 1999). However, the general consensus is that the major impact of ENSO is confined to the Pacific. The MJO tends to be active over the central Pacific and inactive over the western Pacific during a warm ENSO event (Gutzler, 1991; Fink and Speth, 1997). In addition, Waliser *et al.* (1999) found from model experiments that ISO events are very sensitive to small changes in SST and, from the air–sea-interaction point of view, that ISO events might be associated with ENSO.

The current study focuses on the ISO to the west of the dateline and the season from winter to spring. The total kinetic energy during January–May averaged over the region (60–160°E, 5–15°N) (as the ISO over this region is most active – see Li (1991)) shows the possibility of a 2–3-year tendency variation and its association with ENSO events (Figure 9). It appears that the low kinetic energy ( $\leq -0.5 \sigma$ ) associated with these two modes is strongly related to warm ENSO events, and active ISO (kinetic energy  $\geq 0.5 \sigma$ ) almost corresponds to the cold ENSO events. This could be further illustrated by the lag correlation between 5-month total Niño–3.4 SST and the kinetic energy during January–May (Figure 10). It seems that the preceding or contemporaneous 5-month total Niño–3.4 SST has a strong influence on the kinetic energy of both 10–20-day and 30–60-day modes because of the high negative correlation values, ranging from  $-0.47$  to  $-0.74$ . Another important feature is that the 30–60-day mode (or MJO) may have a positive impact on the coming ENSO event, with the correlation coefficient around 0.30 when the kinetic energy leads the Niño–3.4 SST by several months, even though the values are not significant above the 95% confidence level (the critical value is 0.42). On the contrary, 10–20-day mode has no contribution to the occurrence of ENSO events since the coefficient correlation values are almost 0 when the Niño–3.4 SST lags behind.

Note from Figure 10 that the ISO activities over the Indian Ocean and SCS region prior to the monsoon onset seem to be more active in cold ENSO years, and inactive in warm ENSO years. Teng and Wang (2003) use the vertical wind shear to explain the relationship between ISO over western North Pacific and ENSO because there is weak easterly shear over the western Pacific. During a warm ENSO event, the warming in the central and eastern Pacific could induce westerly anomalies in the lower troposphere and easterly anomalies in the upper troposphere over the western Pacific. Some results suggested that zonal vertical shear has a remarkable impact on the development of westward-propagating mixed Rossby–gravity waves (Wang and Xie, 1997; Xie and Wang, 1996). Teng and Wang (2003) found that easterly vertical shears can enhance Rossby wave in the lower troposphere. However, there is no obvious decrease or increase in easterlies over

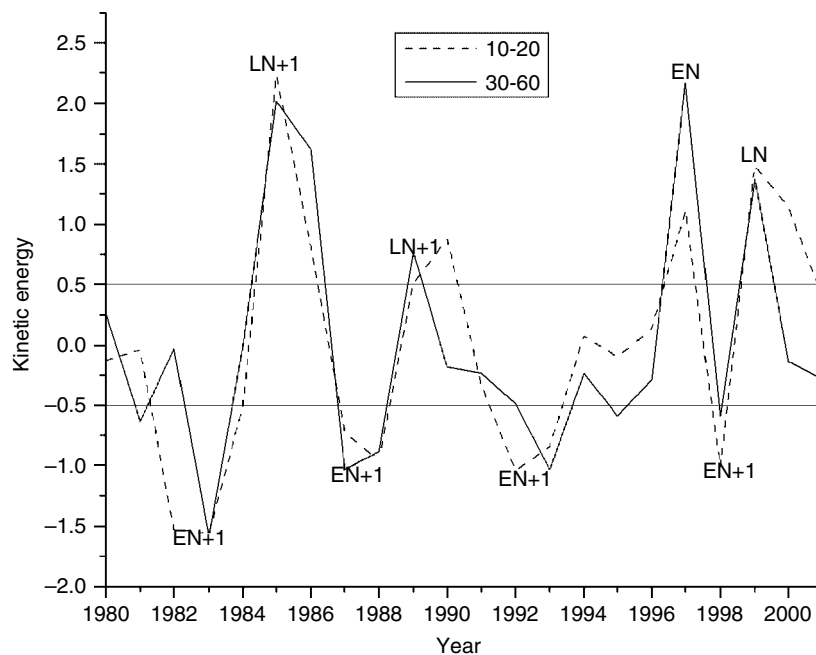


Figure 9. Normalized January–May kinetic energy (10–20-day mode (dashed), 30–60-day (solid)) averaged over (60–160°E, 5–15°N)

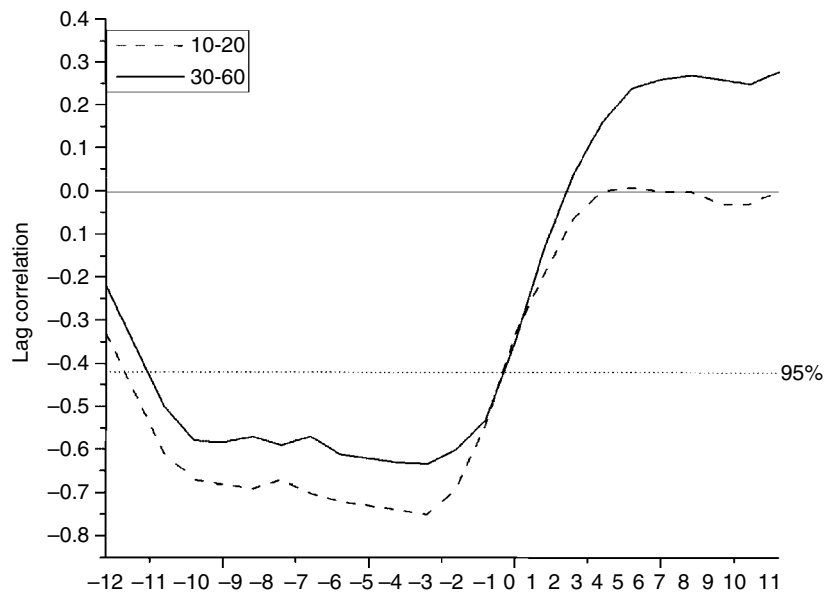


Figure 10. Lag correlation between 5-month total Niño-3.4 SST anomalies and the kinetic energy anomalies of 10–20-day (dashed) and 30–60-day (solid) modes during January–May. Lag 0 refers to the contemporaneous correlation between the Niño-3.4 SST and kinetic energy. Negative (positive) time refers to the Niño-3.4 SST leading (lagging) the kinetic energy. Dotted line indicates the 95% significance level

the Indian Ocean and SCS region during cold or warm ENSO events. On the contrary, during some cold ENSO events, it appears that westerlies prevail over the SCS domain in late April or early May, so that the SCSSM onset tends to occur earlier, and thus the SCS ISO might be strengthened.

Therefore, during a warm ENSO event, the ISO activities turn to be active over the central and eastern Pacific, but inactive over the Indian Ocean and SCS domain (Figures 9–10). On the other hand, the SCS ISO appears to be active during a cold ENSO event (Figures 9 and 10). However, this hypothesis still needs to be further tested.

## 6. SUMMARY AND DISCUSSION

### 6.1. Summary

This paper investigates the role of ISOs in the onset of the SCSSM. On the basis of the analyses of data from 1979 to 2001, two major components of the ISO (10–20-day and 30–60-day modes) can be identified. The coupling between these two intraseasonal modes during both the pre-monsoon and monsoon periods of the SCSSM is studied by examining the filtered OLR, low-level winds, apparent heat source and apparent moisture sink from October of a previous calendar year to September of a calendar year (May is the normal onset month of the SCSSM).

The zonal and meridional propagations of the two modes are found to be different, which reflects their different roles in the establishment and development of the SCSSM. The 10–20-day mode has a northwestward propagation and is associated with the weakening of the WPSH, while the 30–60-day mode originates from convection over the equatorial Indian Ocean and propagates northeastward. On the basis of the analyses, a hypothesis is proposed to explain the observed variabilities in the SCSSM onset. When the equatorial Indian Ocean exhibits a 30–60-day mode oscillation, an initially weak convection develops into a large convection band (or monsoon trough). Meanwhile, a convective disturbance of 10–20-day mode is induced when this monsoon trough extends to the western Pacific. These two processes then collaborate to cause a weakening of the subtropical anticyclone over the SCS. Because the monsoon trough of the 30–60-day mode subsequently

propagates northward into the BOB, the induced vortex together with the 10–20-day westward-migrating convection from the equatorial western Pacific will substantially increase the effect of horizontal advection of moisture and heat, thus destabilizing the atmosphere and weakening the subtropical ridge there. Westerlies can then penetrate and prevail over the SCS region, and the SCSSM onset occurs. Therefore, the ISO leads to the onset of the SCSSM. Moreover, both modes, in particular the 10–20-mode, could modulate the evolution of the SCSSM because the WPSH occasionally extend into the SCS. To some extent, the onset/end cycle and active/break cycle of the SCSSM are due to the coupling of the intraseasonal variabilities. However, it should be noted that for certain years, it is difficult to predict the onset timing of the SCSSM because no large difference can be found between the early and late onset cases.

## 6.2. Discussion

The results in this paper demonstrate that the timing of the SCSSM onset is primarily determined by the phase-locking of 10–20-day and 30–60-day modes. Blade and Hartmann (1993) suggested a ‘charge–recharge’ analog to the instability of the tropical atmosphere. That means the atmosphere requires a certain period of time to ‘recharge’ its instability. Thus, the life cycle of the SCSSM may be explained by ‘charge–discharge–recharge’ of convection over the southern Indian Ocean (30–60-day mode) and that over the equatorial western Pacific (10–20-day mode) working together, which also agrees well with Li’s (1991) ‘CISK–Rossby wave’ resulting from convective heating accompanying both westward and eastward movements of low frequency oscillations in the tropical atmosphere. The moisture convergence over the SCS should therefore have a direct contribution to the SCSSM onset. As we know, three branches of strong low-level westerlies contribute to the development of EASM; the first branch is the strong low-level westerly flow from the Arabian Sea (Somali jet) to southwest China. The second branch is the 105°E, cross-equatorial southwesterly flow and the third branch is the southeasterly flow from the southern flank of the subtropical high over the western Pacific. With the combinations of these three branches of Asia summer monsoon, the dynamic or the thermodynamic conditions and some physical processes of the seasonal march of the EASM become more complicated. The SCS is just a huge water tank, and water due to evaporation or outflow must be replenished at regular intervals (e.g. 10–20-day or 30–60-day).

However, the result of the lag-regression between tropical convection and circulation should be interpreted carefully because only linear relationship is being considered here, and the effect of ENSO is complicated and needs further investigation. For example, owing to the nonlinearity of moist processes, a small rise in SST over the warm pool region will enhance the equivalent heat content of air more rapidly and result in enhanced convection (Webster, 1983). And such a small rise in SST might have a stronger impact on convection, and thus convection could increase with SST, which might lead to above-normal convection over the equatorial Indian Ocean or the western Pacific, resulting in the oscillatory behavior of the 30–60-day and 10–20-day modes (Lau *et al.*, 1997).

## ACKNOWLEDGMENTS

The authors would like to thank the US National Centers for Environmental Prediction for providing the monthly global reanalysis data (1979–2001), the National Oceanic and Atmospheric Administration for the OLR data (1979–2001).

The work of the first author forms part of her Ph.D. work, which was supported by a Research Studentship from City University of Hong Kong. This research is partially supported by the City University of Hong Kong Research Grant No.7001336.

## REFERENCES

- Annamalai H, Slingo JM. 2001. Active/break cycles: diagnosis of the intraseasonal variability of the Asian summer monsoon. *Climate Dynamics* **18**: 85–102.  
Blade I, Hartmann DL. 1993. Tropical intraseasonal oscillations in a simple nonlinear model. *Journal of the Atmospheric Sciences* **17**: 2922–2939.

- Chan JCL, Ai W, Xu J. 2002. Mechanisms responsible for the maintenance of the 1998 South China Sea summer monsoon. *Journal of the Meteorological Society of Japan* **80**: 1103–1113.
- Chang C-P, Lim H. 1988. Kelvin wave-CISK: a possible mechanism for 30-50 day oscillations. *Journal of the Atmospheric Sciences* **45**: 1709–1720.
- Chelliah M, Schemm JE, van den Dool HM. 1988. The impact of low-latitude anomalous forcing on local and remote circulation: winters of 1978/79-1986/87. *Journal of Climate* **1**: 1138–1152.
- Chen TC, Chen JM. 1993. The 10–20-day mode of the 1979 Indian monsoon: Its relation with the time variation of monsoon rainfall. *Monthly Weather Review* **121**: 2465–2482.
- Chen TC, Chen JM. 1995. An observational study of the South China Sea monsoon during the 1979 summer: onset and life cycle. *Monthly Weather Review* **123**: 2295–2318.
- Chen TC, Yen MC, Murakami M. 1988. The water vapor transport associated with the 30-50 day oscillation over the Asian monsoon regions during 1979 summer. *Monthly Weather Review* **116**: 1983–2002.
- Chen TC, Yen MC, Weng SP. 2000. Interaction between the summer monsoon in East Asia and the South China Sea: intraseasonal monsoon modes. *Journal of the Atmospheric Sciences* **57**: 1373–1392.
- Fink A, Speth P. 1997. Some potential forcing mechanisms of the year-to-year variability of the tropical convection and its intraseasonal (25–70 day) variability. *International Journal of Climatology* **17**: 1513–1534.
- Gutzler DS. 1991. Interannual fluctuations of intraseasonal variance of near-equatorial zonal winds. *Journal of Geophysical Research* **96**: 3173–3185.
- Hendon HH, Zhang C, Glick JD. 1999. Interannual variation of the Madden-Julian oscillation during austral summer. *Journal of Climate* **12**: 2538–2550.
- Kessler WS, McPhaden MJ. 1995. Oceanic equatorial waves and the 1991–1993 El Niño. *Journal of Climate* **8**: 1757–1774.
- Krishnamurti TN, Bhalme HN. 1976. Oscillations of a monsoon system. Part I: observational aspects. *Journal of the Atmospheric Sciences* **33**: 1937–1954.
- Krishnamurti TN, Ardanuy P. 1980. The 10–20-day westward propagating mode and break in the monsoon. *Tellus* **33**: 15–16.
- Krishnamurti TN, Subrahmanyam D. 1982. The 30-50 day mode at 850 mb during MONEX. *Journal of the Atmospheric Sciences* **39**: 2088–2095.
- Lau KM, Chan PH. 1986. Aspects of the 40-50 day oscillation during the northern summer as inferred from outgoing longwave radiation. *Monthly Weather Review* **114**: 1354–1367.
- Lau KM, Yang S. 1997. Climatology and interannual variability of the southeast Asian summer monsoon. *Advances in Atmospheric Sciences* **14**: 141–162.
- Lau KM, Wu HT, Bony S. 1997. The role of large scale atmospheric circulation in the relationship between tropical convection and sea surface temperature. *Journal of Climate* **10**: 381–392.
- Li C. 1991. *Low-Frequency Oscillations in the Atmosphere*. Meteorology Publishers: Beijing, China 207 (in Chinese).
- Liu YM, Wu GX, Liu H, Liu P. 2001. Condensation heating of the Asian summer monsoon and the subtropical anticyclone in the Eastern Hemisphere. *Climate Dynamics* **17**: 327–338.
- Liu YM, Chan JCL, Mao JY, Wu GX. 2002. The role of Bay of Bengal convection in the onset of the 1998 South China Sea summer monsoon. *Monthly Weather Review* **130**: 2731–2744.
- Madden RA, Julian PR. 1971. Detection of a 40-50 day oscillation in the zonal wind in the tropical Pacific. *Journal of the Atmospheric Sciences* **28**: 702–708.
- Madden RA, Julian PR. 1972. Detection of global-scale circulation cells in the tropics with a 40-50 day period. *Journal of the Atmospheric Sciences* **29**: 1109–1123.
- Mao JY, Chan JCL. 2005. Intraseasonal variability of south China sea summer monsoon. *Journal of Climate* **18**: 2388–2402.
- Matthews AJ, Kiladis GN. 1999. The tropical-extratropical interaction between high-frequency transients and the Madden-Julian oscillation. *Monthly Weather Review* **127**: 661–677.
- McPhaden MJ. 1999. Genesis and evolution of the 1997-1998 El Niño. *Science* **283**: 950–954.
- Murakami T. 1980. Empirical orthogonal function analysis of satellite-observed outgoing longwave radiation during summer. *Monthly Weather Review* **108**: 205–222.
- Murakami T, Chen L-X, Xie A. 1986. Relationship among seasonal cycles, low-frequency oscillations, and transient disturbances as revealed from outgoing longwave radiation data. *Monthly Weather Review* **114**: 1456–1465.
- Mureau R, Opsteegh JD, Winston JS. 1987. Simulation of the effects of tropical heat sources on the atmospheric circulation. *Monthly Weather Review* **115**: 856–870.
- Nitta T. 1987. Convective activities in the tropical western Pacific and their impacts on the Northern Hemisphere summer circulation. *Journal of the Meteorological Society of Japan* **65**: 165–171.
- Rodwell MR, Hoskins BJ. 2001. Subtropical anticyclones and summer monsoons. *Journal of Climate* **14**: 3192–3211.
- Simmons AJ. 1982. The forcing of stationary wave motion by tropical diabatic heating. *Quarterly Journal of the Royal Meteorological Society* **108**: 503–534.
- Simmons AJ, Wallace JM, Branstator GW. 1983. Barotropic wave propagation and instability, and atmospheric teleconnection patterns. *Journal of the Atmospheric Sciences* **40**: 1363–1392.
- Slingo JM, Rowell DP, Sperber KR, Nortley F. 1999. On the predictability of the interannual behavior of the Madden-Julian oscillation and its relationship with El Niño. *Quarterly Journal of the Royal Meteorological Society* **125**: 583–609.
- Teng H, Wang B. 2003. Interannual variations of the boreal summer intraseasonal oscillation in the Asian–Pacific Region. *Journal of Climate* **16**: 3572–3584.
- Torrence C, Compo GP. 1998. A practical guide to wavelet analysis. *Bulletin of the American Meteorological Society* **79**: 61–78.
- Waliser DE, Lau K-M, Kim JH. 1999. The influence of coupled sea surface temperature on the Madden-Julian Oscillation: a model perturbation experiment. *Journal of the Atmospheric Sciences* **56**: 333–358.
- Wang B, Rui H. 1990. Synoptic climatology of transient tropical intraseasonal convection anomalies: 1975-1985. *Meteorology and Atmospheric Physics* **44**: 43–61.
- Wang B, Xie X. 1997. A model for boreal summer intraseasonal oscillation. *Journal of the Atmospheric Sciences* **54**: 72–86.

- Webster PJ. 1972. Response of the tropical atmosphere to local, steady forcing. *Monthly Weather Review* **100**: 518–541.
- Webster PJ. 1983. Mechanics of monsoon low frequency variability: surface hydrological effects. *Journal of the Atmospheric Sciences* **40**: 2110–2124.
- Wu G, Zhang Y. 1998. Tibetan Plateau forcing and the timing of the monsoon onset over South Asia and the South China Sea. *Monthly Weather Review* **126**: 913–927.
- Wu MLC, Schubert S, Huang NE. 1999a. The development of the south Asian summer monsoon and the intraseasonal oscillation. *Journal of Climate* **12**: 2054–2075.
- Wu GX, Liu YM, Liu P. 1999b. The effect of spatially non-uniform heating on the formation and variation of subtropical high. Part I: scale analysis. *Acta Meteorological Sinica* **57**: 257–263 (in Chinese).
- Xie X, Wang B. 1996. Low-frequency equatorial waves in vertically sheared zonal flows. Part II: unstable waves. *Journal of the Atmospheric Sciences* **53**: 3589–3605.
- Xu J, Chan JCL. 2001. First transition of the Asian summer monsoon in 1998 and the effect of the Tibet-tropical ocean thermal contrast. *Journal of the Meteorological Society of Japan* **79**: 241–253.
- Yasunari T. 1979. Cloudiness fluctuations associated with the Northern Hemisphere summer monsoon. *Journal of the Meteorological Society of Japan* **57**: 227–242.
- Yasunari T. 1981. Structure of an Indian summer monsoon system with around 40- day period. *Journal of the Meteorological Society of Japan* **59**: 336–354.
- Zhu B, Wang B. 1993. The 30–60 day convection seesaw between the tropical Indian Ocean and the western Pacific Ocean. *Journal of the Atmospheric Sciences* **50**: 184–199.